

JRC 2017-2257

HYSTERESIS HEATING OF RAILROAD BEARING THERMOPLASTIC ELASTOMER SUSPENSION ELEMENT

Oscar O. Rodriguez

Mechanical Engineering Department
The University of Texas Rio Grande Valley
Edinburg, TX, 78539, USA
oscar.o.rodriguez01@utrgv.edu

Arturo A. Fuentes, Ph.D.

Mechanical Engineering Department
The University of Texas Rio Grande Valley
Edinburg, TX, 78539, USA

Constantine Tarawneh, Ph.D.

Mechanical Engineering Department
The University of Texas Rio Grande Valley
Edinburg, TX, 78539, USA

Robert E. Jones, Ph.D.

Mechanical Engineering Department
The University of Texas Rio Grande Valley
Edinburg, TX, 78539, USA

ABSTRACT

Thermoplastic elastomers (TPE's) are increasingly being used in rail service in load damping applications. They are superior to traditional elastomers primarily in their ease of fabrication. Like traditional elastomers they offer benefits including reduction in noise emissions and improved wear resistance in metal components that are in contact with such parts in the railcar suspension system. However, viscoelastic materials, such as the railroad bearing thermoplastic elastomer suspension element (or elastomeric pad), are known to develop self-heating (hysteresis) under cyclic loading, which can lead to undesirable consequences. Quantifying the hysteresis heating of the pad during operation is therefore essential to predict its dynamic response and structural integrity, as well as, to predict and understand the heat transfer paths from bearings into the truck assembly and other contacting components. This study investigates the internal heat generation in the suspension pad and its impact on the complete bearing assembly dynamics and thermal profile. Specifically, this paper presents an experimentally validated finite element thermal model of the elastomeric pad and its internal heat generation. The steady-state and transient-state temperature profiles produced by hysteresis heating of the elastomer pad are developed through a series of experiments and finite element analysis. The hysteresis heating is induced by the internal heat generation, which is a function of the loss modulus, strain, and frequency. Based on previous experimental studies, estimations of internally generated heat were obtained. The calculations show that the internal heat generation is impacted by temperature and

frequency. At higher frequencies, the internally generated heat is significantly greater compared to lower frequencies, and at higher temperatures, the internally generated heat is significantly less compared to lower temperatures. However, during service operation, exposure of the suspension pad to higher loading frequencies above 10 Hz is less likely to occur. Therefore, internal heat generation values that have a significant impact on the suspension pad steady-state temperature are less likely to be reached. The commercial software package ALGOR 20.3TM is used to conduct the thermal finite element analysis. Different internal heating scenarios are simulated with the purpose of obtaining the bearing suspension element temperature distribution during normal and abnormal conditions. The results presented in this paper can be used in the future to acquire temperature distribution maps of complete bearing assemblies in service conditions and enable a refined model for the evolution of bearing temperature during operation.

NOMENCLATURE

E''	Loss Modulus [MPa]
P	Power/Unit Volume [W/m^3]
ϵ_A	% Strain
ω	Frequency [Hz]

INTRODUCTION

The elastomer steering pad, which is used in the wheel-axle-bearing assembly of a freight car, as seen in Figure 1, has proved to be extremely beneficial. The purpose of the elastomer pad is to prevent metal-to-metal contact between the bearing adapter and the side frame of the truck. Prior research and experimental studies demonstrate that viscoelastic materials, such as the thermoplastic elastomer suspension element, are known to develop self-heating (hysteresis) under cyclic loading [1]. The hysteresis heating is caused by the internal heat generation of the material element when loaded with an oscillatory load. The internally generated heat then either dissipates through internal molecular mechanisms as heat or remains in the system [2, 3]. If there is no thermal runaway for the heat to dissipate out of the suspension pad, and the pad is being subjected to abnormal frequencies, the internally generated heat is significant and can cause the suspension pad to reach temperatures higher than those of any other component in the truck assembly. Consequently, this may lead to the deterioration and degradation of the suspension pad in the truck assembly and result in mechanical failure.

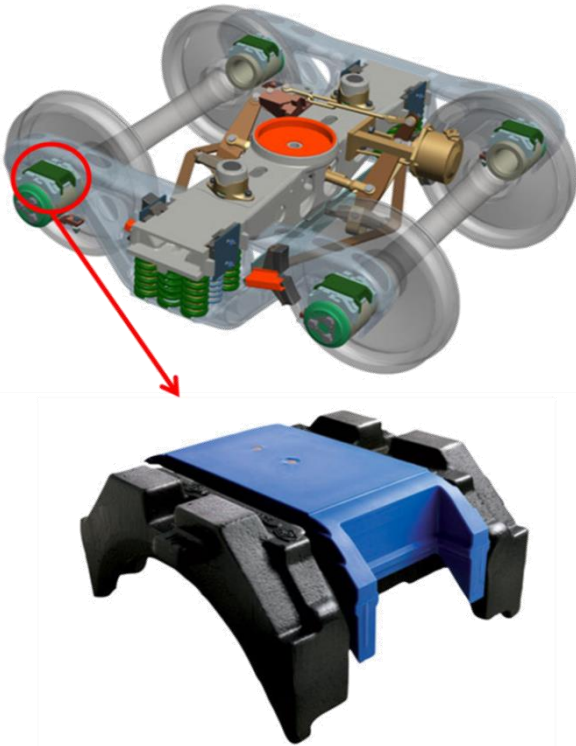


Figure 1. Configuration and location of thermoplastic elastomer steering pad (Blue) within wheel-axle-bearing assembly [4]
Source: <https://www.amstedrail.com/products-services/adapter-plus-steering-pad-system>.

In the following sections, the authors experimentally quantify the internally generated heat in the elastomer suspension pad. These estimated heat generation values were

input, along with other boundary conditions, into an FEA model in order to validate the general approach by comparing FEA predictions with experimental results on cylindrical specimens of pad material. The model is then used to predict the steady state temperature, and the temperature change of the elastomer suspension pad over a defined period of time under various combinations of service loads and conditions. This paper will focus on the thermal behavior of the elastomer suspension pad during both normal and possible abnormal operating conditions, specifically a comparison between the effects of low and high frequency loading over the range from 10 to 50 Hz, which can occur during service. The effects of ambient temperature and equivalent convection coefficients are also studied. These results will help determine the effect of this heat generation on the thermal behavior of railroad bearing assemblies under different operating conditions.

EXPERIMENTAL SETUP & PROCEDURES

Experiments consisted of material characterization using a servohydraulic universal testing system (MTS) and Dynamic Mechanical Analyzer (DMA). The following subsections describe the experimental setups and procedures of both methodologies used to identify the internally generated heat produced by the material specimen when loaded cyclically.

Material Testing System (MTS)

Preliminary findings on the hysteresis heating of the suspension pad were determined by conducting experiments on a 6.3 cm (2.5 in) diameter cylindrical specimen of virgin pad material as seen in Figure 2.



Figure 2. Hysteresis heating cylindrical specimen with thermocouple.

Hysteresis tests were conducted on a MTS 810 Material Testing System with a setup as seen in Figure 3. The setup consisted of the cylindrical specimen mounted in-between two MTS 643 compression platens with a K-class thermocouple inserted fully to contact the center-middle area of the specimen.

The thermocouple is connected to an OMEGA® True RMS SUPERMETER® which displays the temperature of the thermocouple measurement in degrees Celsius. The tests consisted of rapid repeated cycles of compression under loadings ranging between 2.2 kN (500 lbf) and 24 kN (5500 lbf) oscillating at frequencies of 2, 4, 10, 20, 30, and 50 Hertz at room temperature (20°C or 68°F).



Figure 3. Hysteresis heating test setup on MTS 810 Material Test System [5].

Low Frequency Hysteresis Heating

The first set of tests were conducted at loading frequencies of 2, 4, 10, and 20 Hz. The initial temperature was documented at time zero before the test specimen was loaded. Once loaded, temperature measurements were taken every 30 seconds for 5 minutes, followed by every minute for the next 5-10 minutes. A total of 10 minutes of data was collected for 2 and 4 Hz, and 15 minutes of data for 10 and 20 Hz. Multiple tests were run for the same oscillating frequency to check for errors and ensure reliability and repeatability.

High Frequency Hysteresis Heating

The second set of tests were conducted at loading frequencies of 30 and 50 Hz. The initial temperature was documented at time zero before the test specimen was loaded.

Once loaded, temperature measurements were taken every 15 seconds for 2 minutes, followed by every 30 seconds for the next 3 minutes, and finally every minute for the following 10-15 minutes. A total of 15 minutes of data was acquired for 30 Hz, and 20 minutes of data was collected for 50 Hz. Multiple tests were run for the same oscillating frequency to check for repeatability and reliability.

Dynamic Mechanical Analysis (DMA)

The contribution of the elastomer pad to the system energy balance was modeled using data from dynamic mechanical analysis (DMA) of elastomer steering pad material. Specimens were prepared by injection molding as these samples are most representative of the materials in commercially produced pads.

Analysis was performed using a TA Instruments Model Q800 DMA, pictured in Figure 4, running the TA Rheology Advantage software. The instrument allows the specimens to be characterized in different deformation modes (e.g. shear, tension/compression, dual cantilever beam, 3-point bending, and single cantilever). The single cantilever configuration was chosen for this study due to the smaller specimen size required.

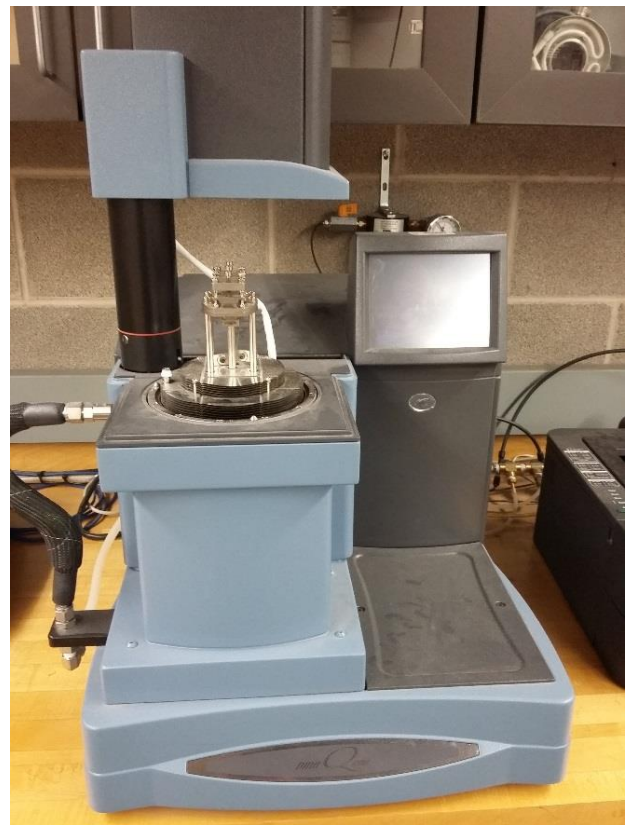


Figure 4. TA Instruments Q800 DMA [6].

Characterization testing consisted of equilibrating the specimen at 30°C for 10 minutes. After that, the first frequency sweep was run. The frequency sweep subjects the sample to an oscillating load at frequencies varying from 0.1 to 50 Hertz. After each frequency sweep is completed, the temperature was

incremented 10°C, held for 10 minutes and then followed by another frequency sweep. The final frequency sweep was performed at 160°C, which is well above the maximum temperature an adapter is likely to see in service operation.

Four different samples were run, each one at a different strain percent: 0.05, 0.50, 2.5, and 12.5; however, for the specimen that was run at 12.5% strain, the frequency range was reduced to 2 Hz due to load and displacement limitations of the instrument used to run DMA experiments.

MTS PRELIMINARY RESULTS

Low Frequency Hysteresis Heating

For loading frequencies of 2, 4, and 10 Hz, the resulting test data sets were neglected due to minimal specimen temperature change (~1-3°C), indicating that regardless of the load magnitude, at frequencies below 10 Hz, the change in the specimen's temperature is not significant for short periods of time (i.e. 10 – 15 minutes). For the loading frequency of 20 Hz, multiple tests were run and the results were fairly similar, having a temperature increase of 5-6°C. Figure 5 displays the comparison curves of the temperature change for the 20 Hz experiments. Both runs for the specimen loaded at 20 Hz show the same trend with approximately a 2°C difference at every timed measurement. The difference seen in the equilibrium temperature is due to a combination of variation in the ambient temperature and the temperature of the contacting surfaces of the test fixtures as well as apparent changes in puck microstructure during cycling which increase the hysteretic effect on subsequent cycles.

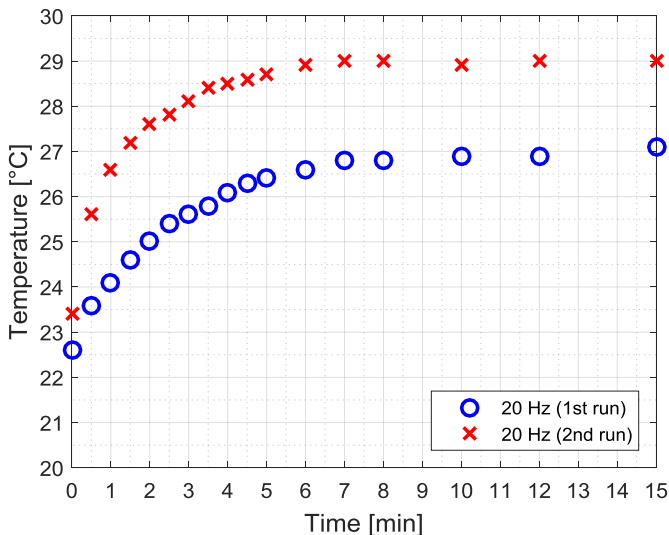


Figure 5. Specimen temperature change loaded at 20 Hz.

High Frequency Hysteresis Heating

Figure 6 displays the comparison curves between the specimen temperature change when exposed to loading frequencies of 30 and 50 Hz. When the specimen is loaded at higher frequencies, it displays a significant increase in temperature. At 30 Hz, the specimen had a temperature increase

of 4°C, and when loaded at 50 Hz, the specimen produced a temperature increase of 12°C. The tests were run again to check for repeatability and reliability of the results. The second set of experiments all showed a higher increase in temperature compared to the first run of experiments. When the specimen was loaded at 30 Hz, it had a temperature increase of 8°C, and at 50 Hz, the specimen had a temperature increase of 22°C. The averages of both runs for each frequency are presented in Figure 7. The average specimen temperature change is used in the model construction.

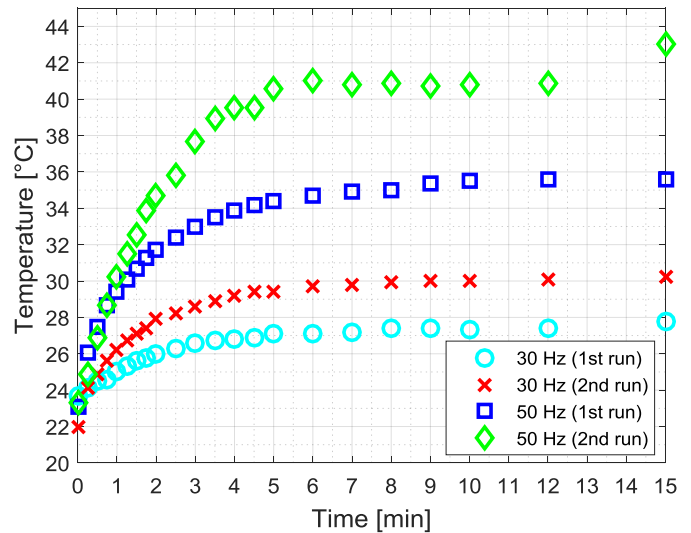


Figure 6. Specimen temperature change loaded at 30 and 50 Hz.

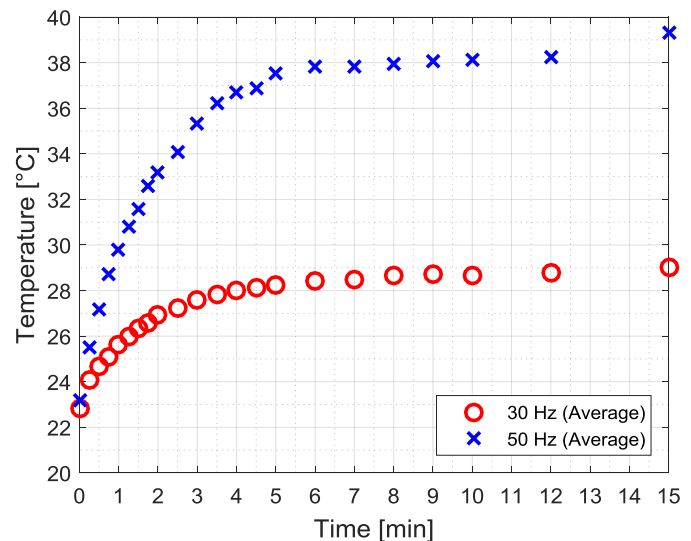


Figure 7. Average specimen temperature change for both runs of 30 and 50 Hz.

DMA HEAT GENERATION QUANTIFICATION

To characterize the elastomeric pad and determine the energy being released by the component, the total heat

generation of the material was numerically estimated using DMA data that was obtained from specimens of the suspension pad material [6]. The data showed that the loss modulus decreases as the specimen temperature increases, meaning that the heat generation will be dependent on temperature and the higher the temperature of the pad the lower the dissipation of energy as heat [6]. Since the heat generation is a function of the loss modulus, strain percent, and frequency, Eq. (1) can be used with DMA results to calculate specific power (W/m^3) dissipated at individual frequencies and temperatures [7].

$$P = \frac{\omega}{2} \epsilon_A^2 E'' \quad (1)$$

For the heat generation calculations, the strain applied in the experiments, 0.05, was used in conjunction with the loss modulus data obtained from the DMA tests. A loading frequency sweep was done on each specimen ranging from 0.1 to 50 Hz; however, heat generation values were calculated only for frequencies of 10, 20, 30, and 50 Hz. The heat generation is also dependent on temperature, and at each frequency, values for the internally generated heat are calculated for temperatures ranging from 30 to 160°C in increments of 10°C. Table 1 and Figure 8 display the heat generation values for all frequency ranges dependent on the temperature.

Table 1. Calculated heat generation values.

Temperature (°C)	50 Hz	30 Hz	20 Hz	10 Hz
	Heat Generation (W/m^3)			
30	14459	8053	4793	2070
40	10441	5842	3394	1428
50	7397	4165	2369	970
60	5065	2910	1615	641
70	3463	2068	1123	428
80	2493	1537	821	300
90	1836	1219	641	228
100	1457	1004	529	184
110	1191	859	455	155
120	1045	808	405	137
130	931	737	375	121
140	873	716	350	111
150	888	748	338	106
160	860	781	313	100

FINITE ELEMENT ANALYSIS

The normal and abnormal operating conditions along with worst-case scenarios are presented in this section. The thermal models presented here focus on normal and abnormal frequency loadings, such as 20 and 50 Hz.

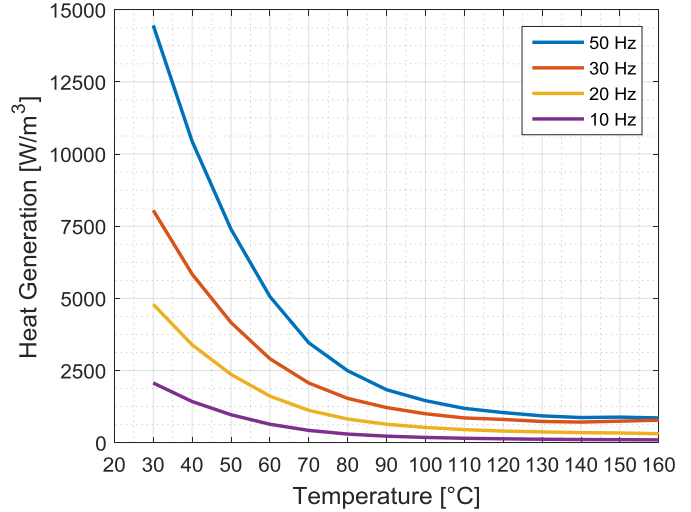


Figure 8. Heat generation curves.

Laboratory Specimen Modeling

An FEA model of the cylindrical specimen, as illustrated in Figure 9, was validated experimentally in order to obtain the steady-state response and the transient response at different time periods. These results allowed us to determine an equivalent overall convection coefficient, which would be an overall estimate of the conduction, radiation, and convection that would yield results close to those seen in the laboratory.

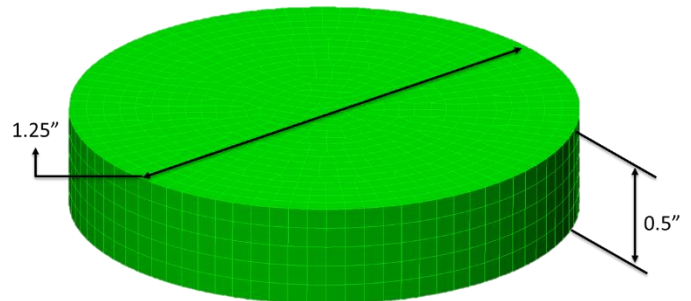


Figure 9. FEA model of hysteresis cylindrical specimen.

First, in order to have reliable results, a sensitivity analysis on the mesh size of the model was run in order to determine whether or not there is convergence of the FEA results. Decreasing the mesh size increases the number of elements and nodes in the model changing the final result every time until the result is similar to that of the exact solution [8]. In essence, the steady-state temperature analysis was used to run the model at different mesh sizes from 100% down to 25% of the original mesh size to compare the resulting temperature. After assuring convergence of the model, a mesh size of 75% was selected using brick elements, which resulted in 7721 elements. To reduce the number of elements, symmetry was taken into consideration, where half of the specimen was used, and later, only quarter of the specimen was used. Another sensitivity analysis on the mesh size was run for each symmetric model, and convergence was assured. The boundary conditions applied

were convection load, heat generation and ambient temperature. Different sensitivity analyses were run to study the dependence of the results on the boundary conditions and to determine an overall convection coefficient, which would be applied to validate the laboratory experiments.

Suspension Pad Modeling

From previous studies conducted on the thermoplastic elastomer steering pad presented in Figure 1, it is known that most of the heat from the adapter is conducted to the central square area on the bottom side of the adapter pad [9]. The FEA model used is the same as the one used in reference [9]; however, the main focus of this paper is the heat generated internally by the steering pad. Sensitivity analyses were carried out to study the dependence of the results on boundary conditions and material properties including elastomer thermal conductivity.

Figure 10 displays the FEA model of the steering pad used for the analysis. A mesh size of 75% was used, the brick element type was selected. The final meshed model consisted of 5248 total elements.

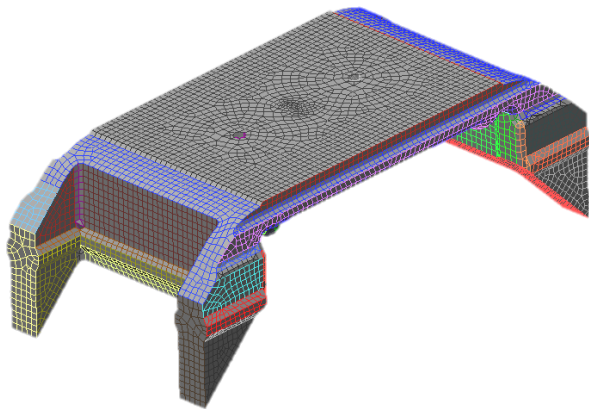


Figure 10. FEA model of thermoplastic elastomer suspension pad.

FEA RESULTS

Both steady-state and transient heat transfer analyses were performed. Properties of the specimen material were sourced from BASF literature TPU using data from grades with the same Shore durometer value. A thermal conductivity of $0.25 \text{ W}\cdot\text{m}^{-1}\cdot\text{K}^{-1}$ along with a mass density of $1160 \text{ kg}\cdot\text{m}^{-3}$ and a specific heat of $2.3 \text{ J}\cdot\text{g}^{-1}\cdot\text{K}^{-1}$ were selected as the specific properties. For the convection coefficient, there is a broad range of values that can be selected; however, a sensitivity analysis was conducted on different convection coefficient values. The heat generation condition was applied as constant homogenous or temperature dependent volume heat generation, in order to determine if the heat generation values that were calculated are reasonable.

Laboratory Specimen

For the initial FEA analysis an overall convection coefficient of $5 \text{ W}\cdot\text{m}^{-2}\cdot\text{K}^{-1}$ was selected. Note that the overall convection coefficient value is representative of all the heat transfer modes (i.e. convection, conduction, and radiation). An ambient temperature of 23.1°C is used. The convection coefficient was selected after a sensitivity analysis was conducted on the steady-state temperature using convection coefficient values from 0.1 to $25 \text{ W}\cdot\text{m}^{-2}\cdot\text{K}^{-1}$. The convection coefficient value which lead to a final temperature similar or close to that of the laboratory specimen was selected as the overall convection coefficient. The analysis was run using the cylindrical specimen FEA model to determine the consistency of the heat generation data. Table 2 summarizes the results of the steady-state temperature of the cylindrical specimen with an applied heat generation produced by a 20 Hz cyclic loading.

Table 2. Steady-state temperature and time of laboratory specimen FEA model with an applied heat generation produced by a 20 Hz cyclic loading.

Heat Generation	Time (min)	Temperature ($^\circ\text{C}$)
Constant	~55	28.05
Temperature Dependent	~55	28.05

The results show that the use of a constant or temperature dependent heat generation model yield the same equilibrium temperature. Both equilibrium temperatures show a similar increase above ambient representative of the approximately 5 degrees measured in the laboratory. In addition, the time it takes to reach the steady-state temperature is approximately the same for both the constant and temperature dependent heat generation models. Since the steady state temperature is below 30 degrees, the FEA analysis of the temperature dependent model only applies the 30 degree heat generation value, which is the same value used in the constant heat generation model. It can be said that the effect of the temperature dependent heat generation does not impact the model for low cyclic loading frequencies such as 20 Hz.

To test for reliability, FEA analysis was conducted using the same specimen now with an applied heat generation produced by a 50 Hz cyclic loading. Table 3 presents the results that exhibit a trend where the constant heat generation case predicts a higher equilibrium temperature. In this case, it takes approximately 25% less time for the temperature to reach steady state using the constant heat generation model. The latter is due to the reduced amount of energy that is being generated at a specific temperature for the temperature dependent heat generation model.

Table 3. Steady-state temperature and time of laboratory specimen FEA model with an applied heat generation produced by a 50 Hz cyclic loading.

Heat Generation	Time (min)	Temperature (°C)
Constant	~46	35.79
Temperature Dependent	~60	35.6

Figure 11 displays the temperature map of the cylindrical specimen with plots of both loading frequencies: 20 and 50 Hz. The figure indicates that the highest temperature is in the center of the cylindrical specimen, and when applying symmetry, it can be seen that the peak temperature is located in the center-middle point of the cylindrical specimen. The center-middle point of the cylindrical specimen is the location where temperature measurements were taken during laboratory testing.

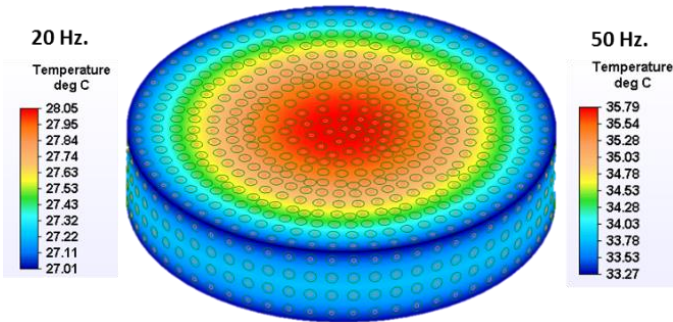


Figure 11. Temperature map of steady-state analysis on cylindrical specimen at frequency loadings of 20 Hz and 50 Hz.

Suspension Pad

Figure 8 clearly demonstrates that the internally generated heat decreases when temperature increases. In order to simulate abnormal conditions for the elastomer suspension pad, only the temperature-dependent heat generation is considered. Using the model illustrated in Figure 10, transient state analysis was conducted for a period of 12 hours. The latter was done in order to represent operating conditions in service during typical running times.

A thermal conductivity of $0.25 \text{ W}\cdot\text{m}^{-1}\cdot\text{K}^{-1}$ along with a mass density of $1160 \text{ kg}\cdot\text{m}^{-3}$ and a specific heat of $2.3 \text{ J}\cdot\text{g}^{-1}\cdot\text{K}^{-1}$ were selected as the specific properties. An average convection coefficient of the pad can be obtained with a minimum air flow of $5 \text{ m}\cdot\text{s}^{-1}$, as calculated in previous studies [8]. This convection coefficient is only applied to those areas completely exposed to the air, and not the top and bottom surfaces that are in direct contact with other components [9]. The applied boundary conditions are: a convection coefficient of $17.9 \text{ W}\cdot\text{m}^{-2}\cdot\text{K}^{-1}$, temperature-dependent heat generation at 50 Hz, and a top and bottom surface applied temperature for both normal and abnormal conditions.

For normal operating boundary conditions, a bottom surface temperature of 50°C was applied. The temperature map of the thermoplastic elastomer suspension pad was obtained for normal operating conditions from previous studies [9]. The study concluded that the bottom surface of the suspension pad conducts most of the heat from the adapter, reaching a temperature of about 50°C . The top surface temperature and ambient temperature were set to be the same, since ideally, most of the heat is dissipated in that direction and for simplification, and the temperature of the surface should be similar to that of the ambient area. Figure 12 shows the temperature distribution map during normal operation. The results show that when a bottom surface temperature of 50°C , and a top surface temperature and ambient temperature of 23.1°C were applied, the peak temperature of the pad reaches 62°C . The peak temperature location is at the center-middle area of the suspension pad.

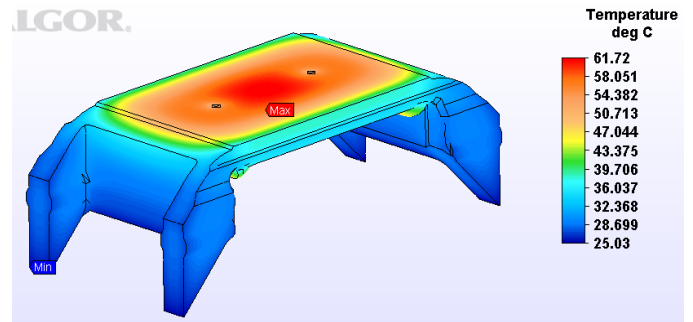


Figure 12. Temperature map of thermoplastic elastomer suspension pad model subjected to normal boundary conditions.

Now, when applying abnormal boundary conditions, such as a bottom surface temperature of 65°C and a top surface temperature and ambient temperature of 45°C , it can be seen from Figure 13 that the absolute temperature of the pad is significantly higher, meaning that the heat generation does have a significant impact on the temperature of the suspension pad which may compromise the structural integrity of the pad past 12 hours of operation.

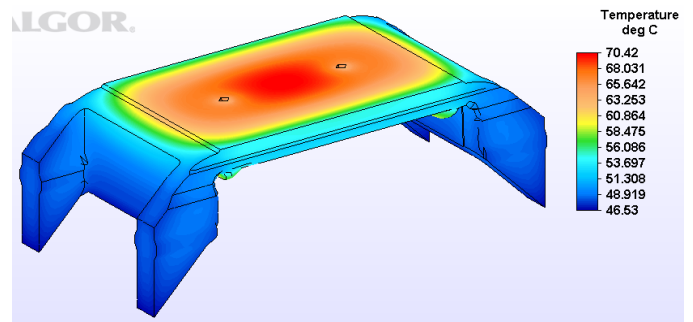


Figure 13. Temperature map of thermoplastic elastomer suspension pad model subjected to abnormal boundary conditions.

To model the worst-case scenario, the steady-state analysis was used. A bottom surface temperature of 85°C along with an ambient and top surface temperature of 45°C, and a constant heat generation were applied as the boundary conditions. Figure 14 shows the resulting temperature map. The peak temperature of the suspension pad under the aforementioned conditions is approximately 137°C, which is clearly above the softening temperature of the pad material.

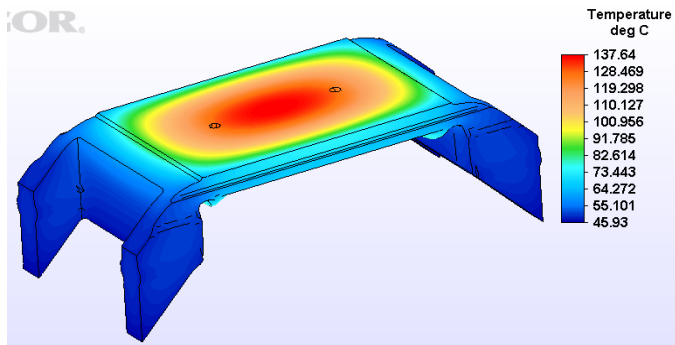


Figure 14. Temperature map of thermoplastic elastomer suspension pad model subjected to worst-case scenario boundary conditions.

CONCLUSIONS

The combination of temperature and frequency dependent material properties with FEA modeling permits the transient modeling and determination of equilibrium temperature of an elastomeric steering pad. Results indicate that the combination of ambient temperatures, bearing temperature, and frequency of loading can produce pad temperature increases above ambient of up to 125°C.

FEA simulations concluded that the worst-case scenario is steady-state loading at ambient temperatures above 45°C with , bearing temperatures above 120°C, and adapter temperature above 85°C. All these thermal effects in conjunction with convection coefficients less $17.9 \text{ W}\cdot\text{m}^{-2}\cdot\text{K}^{-1}$ and constant heat generation can propel elastomer suspension pad temperatures significantly above the softening temperature of the pad material during service operation. When modeling worst-case scenarios, the higher temperature increase occurs at higher loading frequencies such as 50 Hz.

Hysteresis heating is a phenomenon that occurs in service, and may have a significant impact on the structural integrity of the thermoplastic elastomer suspension pad, which can negatively affect the thermal management of the railroad bearing. With proper convection and normal bearing operating conditions, the heat generation will not have a significant effect. However, when a bearing is defective, rail conditions produce high frequency loading, and the ambient temperature is high, the thermoplastic elastomer suspension pad may reach temperatures higher than the softening temperature (i.e. 120°C). The problem is further compounded by the reality that load and thus strain are not uniformly distributed on the pad. Areas

under higher strains will be prone to soften first, reducing the effective area of support, thus, increasing the stress on the unmelted regions, and causing them to soften as well.

FUTURE WORK

Based on the results of this study, the internally generated heat will be applied to the model presented in Figure 15, in order to determine the effect of the heat generation of the thermoplastic elastomer suspension element on the thermal management of the railroad bearing. It is anticipated that the results of this work will provide valuable insight that can be used in the development of future bearing conditioning monitoring systems that incorporate sensors embedded in the thermoplastic elastomer suspension pad element.

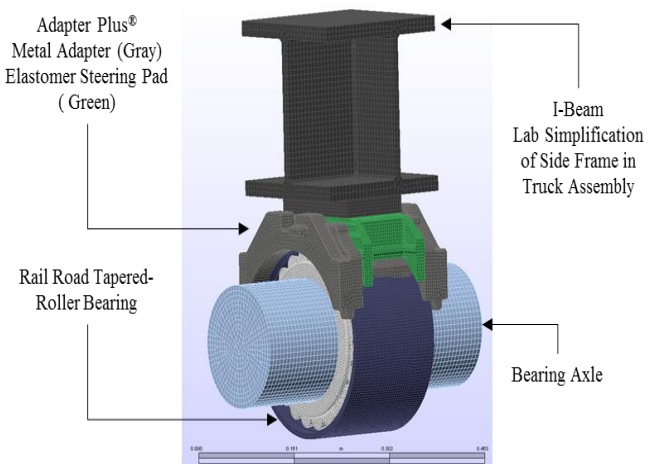


Figure 15. Laboratory test rig FEA model.

ACKNOWLEDGMENTS

This study was made possible by funding provided by The University Transportation Center for Railway Safety (UTCRS), through a USDOT Grant No. DTRT 13-G-UTC59. The authors also gratefully acknowledge the assistance provided by Ms. Samantha Ramirez in the Materials Laboratory. The authors would also like to thank Mr. Juan Carbone, Mr. Daniel Basaldua, and Mr. Anthony Villarreal for their assistance in preliminary data gathering.

REFERENCES

- [1] Rittel, D. An Investigation of the Heat Generated during Cyclic Loading of Two Glassy Polymers. Part I: Experimental. *Mechanics of Materials* 32 (2000): 131-47.
- [2] Rittel, D., N. Eliash, and J.I. Halary. Hysteretic Heating of Modified Poly (methylmethacrylate). *Polymer* 44 (2003): 2817-822.
- [3] Ramkumar, A., K. Kannan, and R. Gnanamoorthy. Experimental and Theoretical Investigation of a Polymer

- Subjected to Cyclic Loading Conditions. *International Journal of Engineering Science* 48 (2010): 101-10. Print.
- [4] Adapter Plus Steering Pad System | Amsted Rail. Web. <http://www.amstedrail.com/adapter-plus-steering-pad-system>
- [5] Basaldua, D. T. Effects of Vapor Grown Carbon Nanofibers on Electrical and Mechanical Properties of a Thermoplastic Elastomer. Master of Science (MS) Thesis, University of Texas-Pan American, Edinburg, Texas, December 2014, 120 pp., 4 Tables, 80 figures, 53 references, 60 titles.
- [6] Rodriguez, O. O., Carbone, J., Fuentes, A. A., Jones, R. E., and Tarawneh, C. Heat Generation in the Railroad Bearing Thermoplastic Elastomer Suspension Element. *Proceedings of the 2016 Joint Rail Conference*, Columbia, SC, April 12-15, 2016.
- [7] Lakes, R. S. *Viscoelastic Solids*. Boca Raton: CRC, 1999.
- [8] Logan, D. L. *A First Course in the Finite Element Method*. Pacific Grove, CA: Brooks/Cole, 2002.
- [9] Zagouris, A., Fuentes, A. A., Tarawneh, C., Kypuros, J. A., and Arguelles, A. P. Experimentally Validated Finite Element Analysis of Railroad Bearing Adapter Operating Temperatures. *Proceedings of the 2012 ASME IMECE Conference*, **IMECE2012-88639**, Houston, TX, November 9-15, 2012.